

## Erosive Burning and its Applications for Performance Prediction

A.R. Kulkarni, K.S. Dalal, P.A. Phawade and P.K. Umrani

*Explosives Research and Development Laboratory, Pune-411 008*

### ABSTRACT

A modified method for prediction of performance of large motors based on erosion constant obtained by partial burning technique is discussed. Erosion constants for two different double base compositions have been determined by partial burning technique. These constants have been used to predict the performance of the large scale motors developed for Defence applications. The predicted performance compares well with the experimental values.

### NOMENCLATURE

|              |   |
|--------------|---|
| $a_0$        | sound velocity, m/s   |
| $a_r$        | burn rate coefficient   |
| $C^*$        | characteristic velocity, m/s  |
| $D_{f_{xm}}$ | final diameter of channel (after burning-time interval $t$ at position $X_m$ , mm)                                      |
| $G$          | mass velocity, kg/s. cm <sup>2</sup>  |
| $G^*$        | critical mass velocity, kg/s. cm <sup>2</sup>   |
| $G_{ratio}$  | $G/G$   |
| $G_{xm}$     | average mass velocity at position $X_m$ (neglecting the density of gas in comparison with that of the solid propellant) |
| $J$          | the ratio of throat area ( $A_t$ ) to port area ( $A_p$ )   |
| $K$          | erosion constant  |
| $K_N$        | the ratio of burning surface-to-throat area   |
| $M$          | Mach number   |
| $M_L$        | Mach number at length $L$   |
| $n$          | pressure index  |
| $P$          | pressure, kgf/cm <sup>2</sup>   |
| $P_0$        | static pressure at $X = 0$  |
| $P_{cal}$    | calculated pressure   |
| $P_s$        | isentropic stagnation pressure  |
| $P_{sna}$    | $P_s/P_0$   |
| $R$          | gas constant = $R_0$ /mol wt  |
| $R_0$        | universal gas constant = $8.314 \times 10^7$ ergs/mole/K  |
| $R_{ratio}$  | $r/r_0$   |
| $R_{xm}$     | time average burning rate at position $X_m$ , mm/s  |
| $r_0$        | burning rate with null gas velocity   |
| $r$          | burning rate with gas velocity  |

|          |   |
|----------|---|
| $T$      | adiabatic flame temperature, K  |
| $V$      | chamber gas velocity, m/s   |
| $X_m$    | distance from fore-end of grain to the aft-end of slice number $m$ , mm |
| $\nu$    | ratio of specific heats   |
| $\rho_p$ | density of propellant, g/cm <sup>3</sup>                                |

### 1. INTRODUCTION

Erosive burning is a common phenomenon experienced in high performance solid propellant rocket motors and generally represents an increase in propellant burning rate due to high velocity combustion gases flowing parallel to the propellant surface. The ability to predict the burning rate is of prime importance in the design of rocket motors, because both the pressure level and burning time depend upon the burning rate. Most propellant grains have a central port through which the combustion gases flow. In such cases the erosive effect is most pronounced in the early stages of propellant combustion, when the ratio of port-to-throat area is small. This erosive effect can lead to large variations in performance of rocket motors since it prevents the grain from burning in parallel layers as is generally assumed for simplicity in performance predictions. The time history of chamber pressure shows discrepancies between theory and experiment. The discrepancies mainly consist of an increase of chamber pressure for a short time after motor ignition and are

due to a local increase in burning rate towards the downstream end of the grain. The flame front reaches the motor casing earlier than predicted and difficulties may be experienced with respect to the heat insulation of the motor hardware in the downstream part of the casing. Thus the erosive effect cannot be eliminated and must be taken into account if one wishes to estimate accurately the performance of propellant and structural resistance of the casing material.

Erosive burning of solid propellants has, therefore, been studied extensively in the past. A comprehensive review of the literature on erosive burning, both theoretical and experimental approaches, was conducted by many authors<sup>1-3</sup>. Experimental approaches to erosive burning can be divided into two major categories; full scale rocket motor test, and small scale laboratory tests on a sample propellant. The partial burning technique which involves simulation of realistic gas-dynamic conditions in the motor, belongs to the first category. Green<sup>4</sup> applied this method to composite propellants. Double base propellants have been widely used in many propulsion applications because they exhibit some superior combustion characteristics such as plateau burning and smokeless combustion.

The prediction of pressure level and burning time depends upon the burning rates which are enhanced in case of high performance rockets for which the ratio of port-to-throat area approaches one. Green<sup>4</sup> has proposed the method for two cases where (i) the gas velocity is low, and (ii) gas velocity varies linearly along the grain length. It has been proved that this method is applicable for high values of port-to-throat area ratios (generally  $A_p/A_t > 2$ ) which reduce the accuracy in the pressure drop correction.

Blatz<sup>5</sup> has worked out an analytical expression for the erosion constant in terms of maximum pressure realised in static test, pressure index and theoretically calculated pressure. This method holds good only when  $A_p/A_t > 2$  and fails to predict the pressure-time profile accurately in the case where port-to-throat area ratio is around unity. Tutoms, *et al*<sup>6</sup> have attempted to predict the pressure-time profile by considering the velocity effect on erosive burning. They have applied the method to both fast burning and slow burning propellants. However, it has been observed that this method fails to predict the initial peak pressure in the case where the port-to-throat area ratios are around unity.

The objectives of the study were to (i) develop experimental facilities, (ii) study the erosive burning phenomenon, and (iii) to propose a modified method for the performance prediction of double base propellant motors. This study is useful to predict the performance of these propellants where there is a possibility of erosive burning.

## 2. EXPERIMENTAL DETAILS

In this method the combustion process is interrupted abruptly, after a certain duration of the time. The interruption is achieved by quickly opening the fore-end of the rocket casing in order to produce a sudden release of the combustion gases. The cover plate sealing of the fore-end of the chamber is secured by two split discs. Prior to firing, the discs are held in place by an adhesive cloth tape. A suitable primacord is wrapped in the groove under the discs. In the operation, a detonator set off electrically at a predetermined time, is used to ignite the primacord, which in turn blows off the split discs. The chamber pressure then ejects the fore end cover and the pressure falls. The grain, extinguished by this rapid depressurisation and its concurrent cooling action, gets ejected from the chamber into a tank of water which prevents reignition. The grain is inhibited externally on lateral surfaces along with the end surfaces. The partially burnt grain is recovered and cut into pieces (slices) of 25.4 mm length; measurements of internal diameters of the fore-end and aft-end of each section are carried out at two positions 90° apart.

## 3. MATHEMATICAL ASPECTS

For this study the mathematical model used is

$$r/r_0 = 1 + k(G/G^*),$$

where  $k$  is erosion constant.

The average mass velocity at different points along the grain was computed by the mass balance equation (neglecting the density of gas in comparison with that of the solid propellant) for one-dimensional flow<sup>7</sup>

Critical mass-velocity

$$G^* = [ \nu + 1 \times (P_0^2 / 2RT$$

$$P/P_0 = (1/(\nu+1) + (\nu/\nu+1)) [1 - (G/G^*)^2]^{1/2} \quad (3)$$

$$G/G^* = (M/(1+\nu M^2)) [2(\nu+1) / (1+(\nu-1)/2 M^2)]^{1/2} \quad (4)$$

$$T/T_0 = [1 + ((\nu-1)/2) M^2]^{-1} \quad (5)$$

$$P/P_0 = [1 + ((\nu-1)/2) M^2]^{(\nu/(\nu-1))} / (1+\nu M^2) \quad (6)$$

$$V/a_0 = M [1 + ((\nu-1)/2) M^2]^{-1/2} \quad (7)$$

Using the above expressions, the pressure, temperature and velocity distributions along the grain were computed. The zero velocity burning rate  $r_0$  at each position was determined from the fore-end burning rate by a correction for the change due to pressure drop along the grain. The ratio  $r/r_0$ , called the erosion function, is plotted against  $G/G^*$  in Fig. 1. The slope of the graph gives the value of the erosion constant  $K$ .

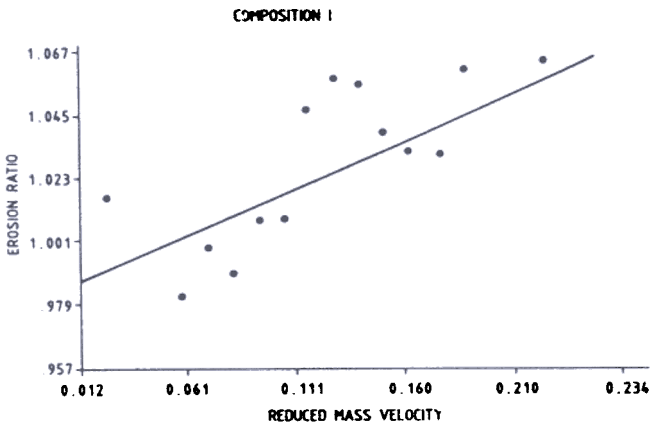


Figure 1. Erosion ratio vs reduced mass velocity.

#### 4. PERFORMANCE PREDICTION

This comprises of predicting the time history of motor pressure and thrust by using theoretical performance parameters based on thermochemical calculations. Each of these two profiles consists of three parts, viz. the initial pressure rise, the steady state curve, and the tail-off curve. The propellant characteristics, the burning rate spectrum in particular, determine the performance profiles.

##### 4.1 The Proposed Model :

The method employs Eqn (1) as the basis. The erosion constant  $K$  has been obtained by partial burning

technique. This model accounts for both pressure and velocity effect on erosive burning rate. Using the continuity equation, we get

$$P_0 = \frac{a \rho_p C^*}{g} K_N \frac{(1+\Gamma^2 J^2)}{(1-\frac{1}{2}\Gamma^2 J^2)} (\sqrt{\nu} M_L)^{-n} (\tan^{-1}(\sqrt{\nu} M_L))^n \left(1 + \frac{2k}{(\nu-1)M_L}\right) \quad (8)$$

In order to derive this equation, the following equations were used:

$$P_{ar} = \frac{1}{L} \int_0^L P dx \quad (9)$$

$$r_{ar} = \frac{1}{L} \int_0^L r dx \quad (10)$$

$$r = a P_0^n (\sqrt{\nu} M_L)^{-n} (\tan^{-1}(\sqrt{\nu} M_L))^n \left(1 + K \frac{G}{G^*}\right) \quad (11)$$

$$r_{ar} = \frac{a P_0^n}{L} (\sqrt{\nu} M_L)^{-n} (\tan^{-1}(\sqrt{\nu} M_L))^n \int_0^L \left(1 + K \frac{G}{G^*}\right) dx \quad (12)$$

This method uses the effective  $K$  ratio and  $G/G^*$  ratio. The prediction given by this method is in good

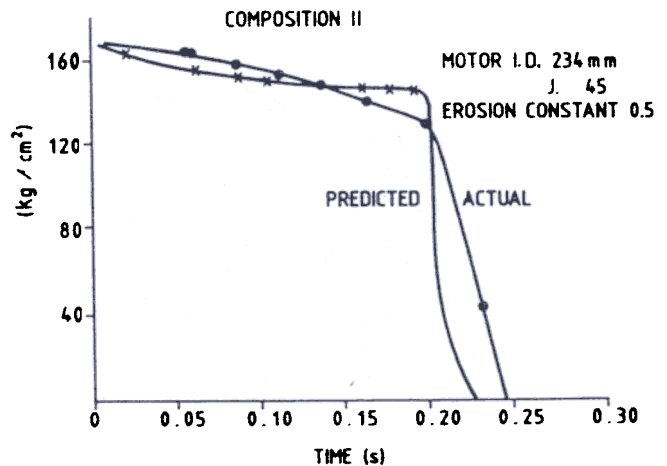


Figure 2. Comparison of predicted and actual pressure-time profile.

agreement with the experimental profiles, as would be seen from Fig. 2.

5. RESULTS AND DISCUSSION

Thermochemical properties of the combustion products of these propellants are presented in Table 1.

Table 1. Thermochemical properties of combustion products

| Property                    | Composition I      | Composition II    |
|-----------------------------|--------------------|-------------------|
| <b>Chemical composition</b> |                    |                   |
| Ingredient                  | Percentage         | Percentage        |
| NC (12.2%)                  | 57.63              | 58.00             |
| NG                          | 27.30              | 29.80             |
| DBP                         | 4.54               | 6.80              |
| 2N-DPA                      | 1.39               |                   |
| DNT                         | 5.98               |                   |
| Chalk                       | 1.87               |                   |
| Magnesium oxide             | 1.05               |                   |
| Cobalt oxide                | 0.33               |                   |
| Zink stearate               | 0.05               |                   |
| C/wax                       | 0.05               |                   |
| Carbamite                   |                    | 2.90              |
| Lead stearate               |                    | 2.00              |
| C/black                     |                    | 0.50              |
| Density                     | 1.59               | 1.57              |
| Burning rate Law            | $r = 0.11P^{0.44}$ | $r = 0.4P^{0.82}$ |
| Adiabatic flame temp(K)     | 2265               | 2129              |
| Specific heat ratio         | 1.249              | 1.259             |
| C* (m/s)                    | 1337               | 1334              |
| Molecular weight            | 24                 | 22.65             |

The experimental curves of chamber pressure vs time obtained from interrupted burning tests of propellants are presented in Fig. 3. These curves are typical of the pressure-time records obtained with an internal burning tubular charge of a propellant.

The experimental data of burning rate vs mass velocity observed in these tests are presented in Fig. 4. The mass flow rates observed in these tests are presented in Fig. 5, as a function of the distance from the fore-end of the grain; the non-linearity observed there manifests the erosive burning effect.

These tests recorded average pressures varying from 59 to 144 kgf/cm<sup>2</sup>. For Composition I, port-to-throat area ratio is of the order of 1.87, whereas in the Composition I, the same is 3.57. Consequently, the first

composition shows more erosion than the second one. In all the tests for the Composition I at the time of interruption, Mach number varies from 0.2 to 0.3 showing 15 percent erosion at 0.3 Mach. This in turn establishes the value of threshold velocity which is of the order of 150 m/s as reported in literature for Composition I. In the case of Composition II, the threshold velocity is of the order of 100 m/s. The values of erosion constants calculated by the method of least squares are appended in Table 2.

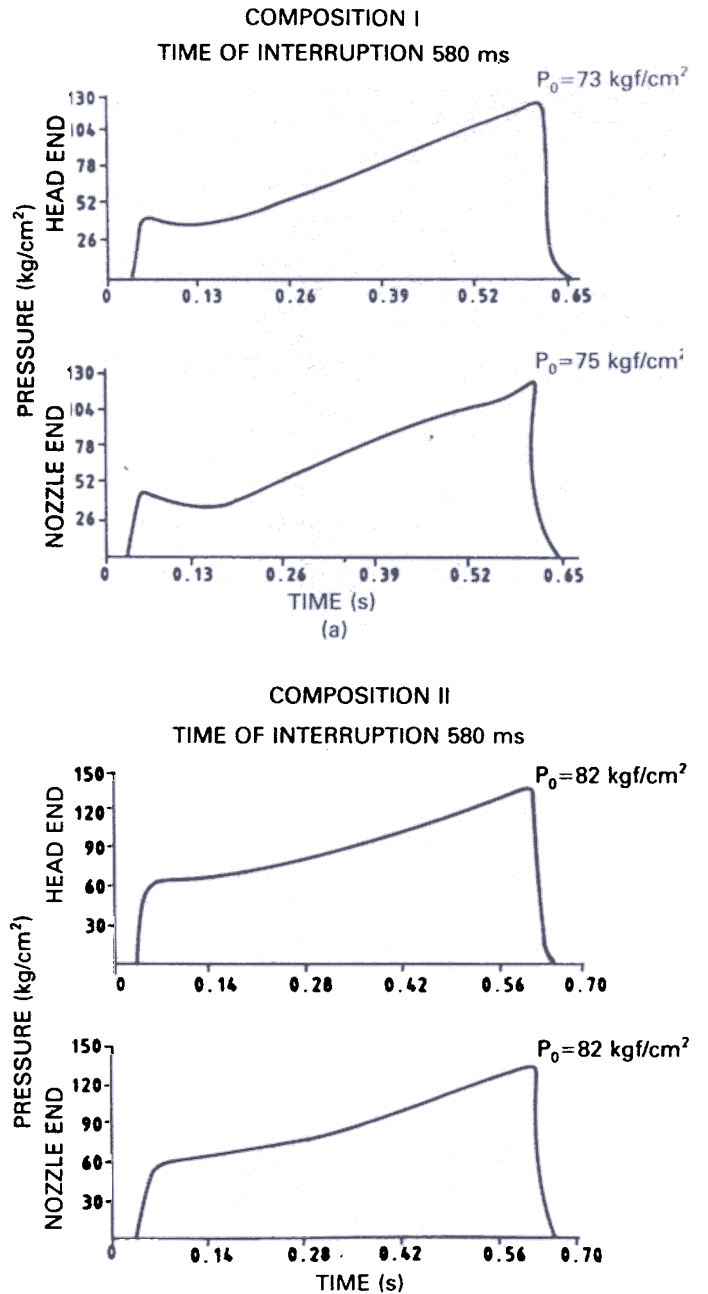


Figure 3. Curves of chamber pressure vs time from interrupted burning tests of the propellants.

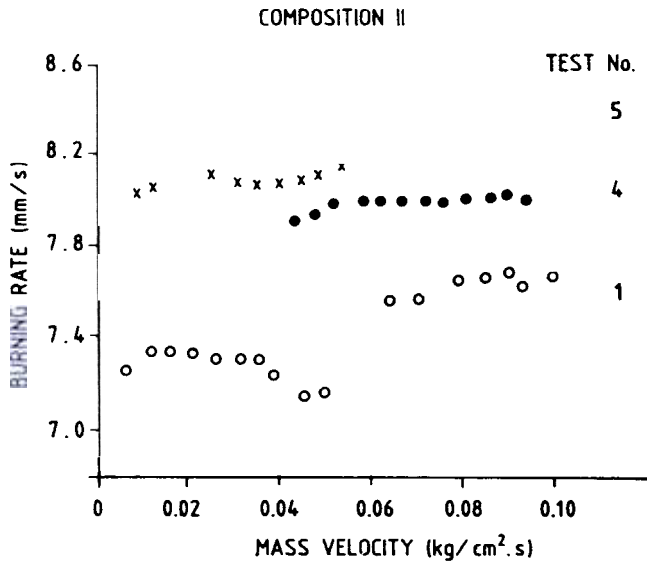


Figure 4. Time average burning rate vs time average mass velocity.

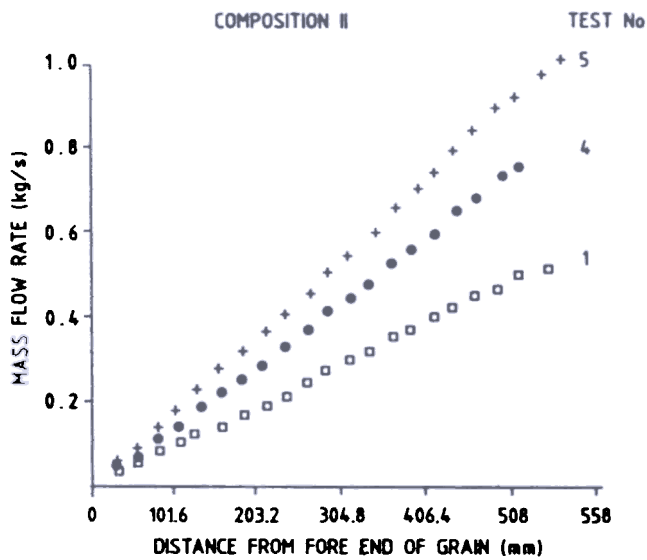


Figure 5. Mass flow rate vs distance from fore-end of grain.

It is evident from Fig.1 that the data are not correlated in terms of mass velocity and also that in order to compensate for differences in pressure level

prevailing during the different tests, a correlation in terms of either linear velocity or reduced mass velocity is required. The data on other propellants studied showed the same behaviour. In this connection, it was noted that the erosive burning data for JPN ballistite and a German double, base propellant presented by Wimpress<sup>8</sup> deviated markedly from the linear expression showing at high velocities, a curvature concave downward when plotted in terms of  $r/r_0$ . Similar curvature was exhibited by the one-dimensional gas dynamic relationship between reduced mass and Mach number as shown in Fig. 6. This justifies the choice of the relationship given by Eqn (1) as can be seen in Fig. 1.

Figure 6 supports the trend observed by Wimpress<sup>8</sup>, i.e., the linear approximation in terms of  $G/G^*$  is preferred for the design of high performance motors with  $J \approx 1$ . The Fig.7 describes the effect of  $G/G^*$  on various ratios. From the data given in Table 2 and computed data presented in Table 3, it is evident that the erosive burning effect is more pronounced in slow burning propellants than in the fast burning ones. This dependence has long been known. A similar general trend for composite propellants is concluded by Green<sup>4</sup>.

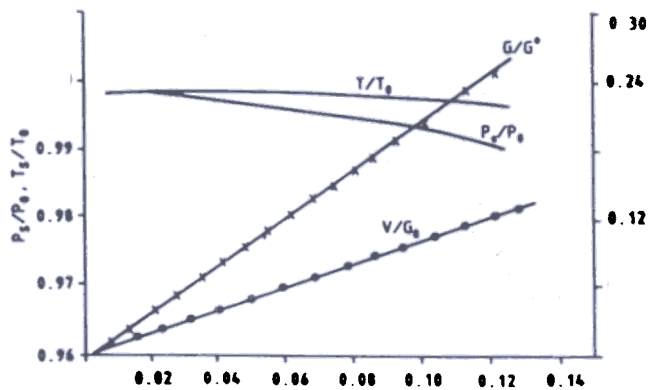


Table 2. Data on erosion constant by partial burning technique

| Test No. | K             |                | Time of interruption (ms) |                |
|----------|---------------|----------------|---------------------------|----------------|
|          | Composition I | Composition II | Composition I             | Composition II |
| 1        | 0.296         | 0.14           |                           | 225            |
| 2        | 0.305         | 0.14           |                           | 380            |
| 3        | 0.321         | 0.14           |                           | 470            |
| 4        | 0.299         | 0.14           |                           | 580            |
| 5        | 0.340         | 0.14           |                           | 670            |



Table 3. Computed values of data from Table 2

| Composition I                                   |  |  |  |  | Test No. 2                              |  |  |  |
|---|--|--|--|--|---|--|--|--|
| Grain dimensions                                |  |  |  |  | Gas properties                          |  |  |  |
| Outer dia, $D = 62$ mm                          |  |  |  |  | Adiabatic flame temp. = 2265° K         |  |  |  |
| Inner dia, $d = 23.39$ mm                       |  |  |  |  | Gas density = 0.00191 g/cm <sup>3</sup> |  |  |  |
| $P_o = 63.31$ kg/cm <sup>2</sup> , $L = 620$ mm |  |  |  |  | Molecular wt. = 24.06                   |  |  |  |
| Time of interruption = 0.370 s                  |  |  |  |  | $K = 0.305$                             |  |  |  |
|   |  |  |  |  | Specific heat ratio = 1.25              |  |  |  |

| $X_m$ | $D_{fzm}$ | $R_{fzm}$ | $G_{fzm}$ | $P_{cal}$ | $M$  | $P_{stat}$ | $G_{ratio}$ | $R_{ratio}$ |
|-------|-----------|-----------|-----------|-----------|------|------------|-------------|-------------|
| 0.0   | 28.76     | 7.26      | .000      | 0.00      | .000 |            |             |             |
| 25.4  | 28.77     | 7.2       | .004      | 63.31     | .006 |            |             |             |
| 50.8  | 28.84     | 7.37      | .009      | 63.30     | .011 |            |             |             |
| 76.2  | 28.62     | 7.07      | .013      | 63.29     | .017 |            |             |             |
| 101.6 | 28.53     | 6.95      | .018      | 63.27     | .023 |            |             |             |
| 127.0 | 28.65     | 7.11      | .022      | 63.25     | .028 |            |             |             |
| 152.4 | 28.74     | 7.23      | .027      | 63.22     | .034 |            |             |             |
| 177.8 | 28.69     | 7.16      | .031      | 63.19     | .040 |            |             |             |
| 203.2 | 28.79     | 7.3       | .036      | 63.15     | .045 |            |             |             |
| 228.6 | 28.78     | 7.28      | .040      | 63.10     | .051 |            |             |             |
| 254.0 | 28.99     | 7.57      | .045      | 63.06     | .057 |            |             |             |
| 279.4 | 29.04     | 7.64      | .049      | 63.00     | .063 |            |             |             |
| 304.8 | 29.03     | 7.62      | .054      | 62.94     | .069 |            |             |             |
| 330.2 | 29.94     | 7.50      | .059      | 62.87     | .075 |            |             |             |
| 355.6 | 28.90     | 7.45      | .063      | 62.79     | .081 |            |             |             |
| 381.0 | 28.89     | 7.43      | .068      | 62.71     | .087 |            |             |             |
| 406.4 | 29.04     | 7.64      | .073      | 62.63     | .093 |            |             |             |
| 431.8 | 29.12     | 7.74      | .077      | 62.54     | .100 |            |             |             |
| 457.2 | 29.26     | 7.93      | .082      | 62.43     | .106 |            |             |             |
| 482.6 | 29.04     | 7.64      | .087      | 62.33     | .112 |            |             |             |
| 508.0 | 28.49     | 6.89      | .091      | 62.22     | .118 |            |             |             |

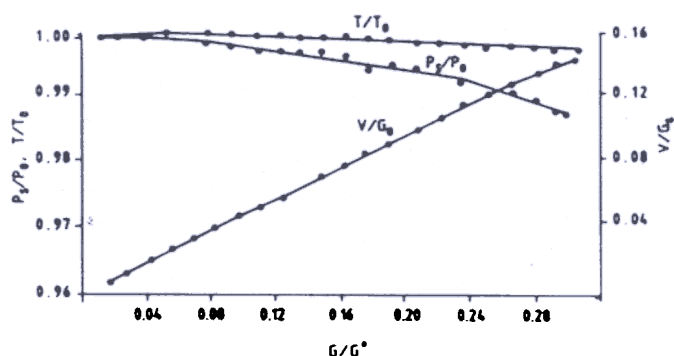


Figure 7. Pressure, temperature and velocity ratio as a function of reduced mass velocity.

The burning surfaces and the port areas were computed using the grain geometry. The propellant characteristics and the burning rate law have been used to evaluate the pressure and time with the help of Eqn (8). The performance prediction using the modified method and the erosion constant has been carried out

for the Composition I and presented in Fig. 2. The peak pressure observed in actual static test compares well with the predicted one. The pressure-time profile obtained in the test shows a close match to the predicted one. The observed deviation in the actual pressure-time profile from the predicted one may be due to the burning rate data obtained using strand burner tests.

## 6. CONCLUSION

A study has been carried out for two double base compositions using the partial burning technique as was done by Green<sup>4</sup>. This method of partial burning technique is useful for determining the erosion constant which signifies the extent to which burning rate can increase due to erosion. Using this erosion constant, performance of large size propellant grains can be predicted to a sufficient accuracy. This erosion constant

plays a significant role in case of high performance rockets with ( $J \approx 1$ ). In such cases, this method of prediction and determination of constant are highly useful.

#### ACKNOWLEDGEMENTS

The authors are grateful to Dr Haridwar Singh, Director, ERDL, for his valuable guidance and suggestions during preparing this paper.

#### REFERENCES

- Razdan, M.K. & Kuo, K.K. Erosive burning study of composite solid propellant by turbulent boundary layer approach. *AIAA Journal*, 1979, **17**, 1225-33.
- 2 King, M.K. A modification of the composite propellant erosive burning model of Lenoir and Robillard. *Combustion and Flame*, 1975, **24**, 365-68.
  - 3 Willams, F.A.; Barriere, M. & Huang N.C. Fundamental aspects of solid propellant rockets. AGARDgraph-116, (Technivision). AGARD, 1969.
  - 4 Green, L. Erosive burning of some composite solid propellants. *Jet Propulsion*, 1954, **24**(1), 9-15.
  - 5 Blatz, P.J. A simplified approach to erosive burning. Paper presented in the 8th Symposium (International) on Combustion, Baltimore, 1961. pp. 745-50.
  - 6 Tutoms, *et al.* A new expression for erosive burning of solid propellants. Second Symposium (International) on Rockets and Astronautics, Tokyo, 1960. pp. 20-25.
  - 7 Shapiro, M. The dynamics and thermodynamics of compressible fluid flow, Vol. 1. Ronald Press, 1955. p. 239.
  - 8 Wimpres, R.N. Internal ballistics. McGraw-Hill, New York, 1950. p. 181.